IR and UV Spectra of the Matrix-Isolated Peroxy Radicals CF_3OO, *trans*-FC(O)OO, and *cis*-FC(O)OO

Stefan Sander, Holger Pernice, and Helge Willner*[a]

Abstract: The peroxy radicals CF_3OO and FC(O)OO are prepared in high yields by vacuum flash pyrolysis of $ROONO_2$ or ROOOR ($R = CF_3$, FC(O)), highly diluted in inert gases, and subsequent isolation in inert-gas matrices by quenching the product mixtures at low temperatures. The IR spectrum of FC(O)OO was observed for the first time and eight fundamentals as well as several combinations were measured and assigned for both *cis* and *trans* rotamers of FC(O)OO. Discrepancies in an earlier assignment of the fundamentals of CF_3OO have been eliminated and its IR spectrum is reported fully. The matrix UV spectra of both peroxy radicals ($X^2A'' \rightarrow 2^2A''$ transition) are in agreement with the gas-phase spectra; however, there are differences in the absorption cross-sections, for which possible reasons are discussed. The $X^2A'' \rightarrow 1^2A'$ transitions in the near IR region are too weak to be detected with our instrumentation.

Keywords: matrix isolation · peroxy radicals · radicals · rotamers · UV/Vis spectroscopy · vibrational spectroscopy

Introduction

The peroxy radicals CF_3OO and FC(O)OO are important and relatively stable intermediate species in the atmospheric photochemistry of alternative halocarbons.[1] They are stable with respect to reaction with the major atmospheric constituents; however, fast reactions occur with trace gases, such as nitrogen oxides and the peroxy radicals HO_2 and CH_3O_2. With HO_2 the corresponding hydroperoxides are formed, and the reaction with NO according to Equation (1) is likely to be the major fate of the CF_3OO and FC(O)OO radicals in the atmosphere.[2–5] In the presence of NO_2, peroxynitrates[6, 7] are formed [Eq. (2)]; these may serve as reservoir species for either ROO or NO_2 radicals.

$$RO_2 + NO \longrightarrow RO + NO_2 \qquad (1)$$

$$RO_2 + NO_2 + M \rightleftharpoons ROONO_2 + M \qquad (2)$$

All recent kinetic studies on the reaction between ozone and CF_3O_x or $FC(O)O_x$ radicals ($x = 0$, 1, 2) have led to the conclusion that these radicals will have only a minor impact on the concentration of stratospheric ozone.[2, 4, 8–11] Considerably before 1990, when the Alternative Fluorocarbon Environmental Acceptability Study (AFEAS programme, supported by 11 companies)[12, 13] was started, the existence of FC(O)OO and CF_3OO radicals had been postulated to interpret the kinetics of some reaction systems. For example, FC(O)OO radicals are important in the thermal reaction of $F_2/CO/O_2$ mixtures that yield FC(O)OOC(O)F[14, 15] and CF_3OO radicals, which are involved in the photochemical reaction of $F_2/CF_3C(O)CF_3/O_2$ mixtures to give CF_3OOOCF_3 and CF_3OOCF_3.[16] First direct spectroscopic evidence for the peroxy radicals in the gas phase was obtained from UV measurements. After laser flash photolysis of $F_2/CO/O_2$ mixtures[17] or pulse radiolysis of $SF_6/CO/O_2$ mixtures,[2] transient species were observed in the 190–310 nm region and, after spectral manipulation, similar spectra of FC(O)OO were obtained for both routes. Absolute absorption cross-sections were obtained from a comparison of the measured FC(O)OO absorbance with that of C_2H_5OO measured under identical conditions, except that CO was substituted by ethane in the flow cell. Analogous flash photolysis/time-resolved UV spectroscopy of $F_2/CF_3H/O_2$ mixtures and pulse radiolysis/transient UV spectroscopy of $SF_6/CF_3H/O_2$ mixtures in a flow cell allowed measurements of the absorption spectrum of CF_3OO.[18, 19]

The IR spectrum of CF_3OO was obtained from several matrix studies.[20–23] Butler and Snelson produced CF_3OO by vacuum pyrolysis of CF_3I followed by co-condensation with oxygen-doped argon at 12 K.[20] Most of the results were confirmed by photooxidation experiments of CF_3I/O_2 in an argon matrix.[21–23] To our knowledge, no experimental IR data of FC(O)OO have been published to date.

In the self-reaction of CF_3OO, the only carbon-containing product observed by FTIR spectroscopy was CF_3OOOCF_3.[19]

---

[a] Prof. Dr. H. Willner, Dipl.-Chem. S. Sander, Dipl.-Chem. H. Pernice
FB6-Anorganische Chemie
Gerhard-Mercator-Universität Duisburg
Lotharstr. 1, 47048 Duisburg (Germany)
Fax: (+49)203-379-2231
E-mail: willner@uni-duisburg.de

0947-6539/00/0619-3645 $ 17.50+.50/0

On the other hand, the stable carbon-containing products of the self-reaction of FC(O)OO were identified as FC(O)OOC(O)F and CO_2.[24, 25] The elusive trioxide FC(O)OOOC(O)F was postulated as a short-lived intermediate.[26]

Further properties of CF_3OO and FC(O)OO were predicted by quantum-chemical computations. The heat of formation ΔH_f^{298} of CF_3OO in the X^2A'' ground state calculated at the MP2/6-316(d,p) level[27] and at MP4 level corrected for bond additivity[28] was found to be -147.8 and -149.8 kcal mol^{-1}, respectively. The molecular structure[27] and vibrational spectrum[28] of CF_3OO was also predicted by the same authors. Isodesmic reactions at the B3LYP/6-311++G(d,p) level of theory yield the enthalpy of formation for FC(O)OO to be -76.1 ± 4 kcal mol^{-1}.[29] In a density functional theory (DFT) study by McKee and Webb it was demonstrated that FC(O)OO in the X^2A'' ground state should exist as a mixture of rotamers [Eq. (3)], whereby *trans*-FC(O)OO is 0.6 kcal mol^{-1} more stable than *cis*-FC(O)OO. In addition, the molecular structures and IR spectra of both rotamers were calculated.[30]

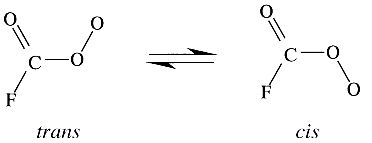

(3)

In order to gain more experimental evidence for the three interesting species CF_3OO, *trans*-FC(O)OO and *cis*-FC(O)OO, we decided to perform a matrix-isolation study in order to:

1) measure the unknown IR spectra of the FC(O)OO rotamers,
2) detect their unknown electronic absorption spectra in the near-infrared region,
3) remove some discrepancies in the assignment of the observed fundamentals of CF_3OO and
4) check the UV spectra of both peroxy radicals by an independent method.

Matrix-isolated radicals can be produced in excellent yields by vacuum flash pyrolysis of thermally labile precursors, highly diluted in argon or neon, followed by quenching the products as a matrix at low temperatures. Recent examples are FCO_2[31] and ClO_3,[32] formed by dissociation of the precursors FC(O)OOC(O)F and $ClOClO_3$, respectively. Suitable thermally labile precursors for the syntheses of the peroxy radicals XOO ($X = CF_3$, CFO) are the peroxy nitrates $XOONO_2$ ($X = CF_3$,[7] FCO[6]) and the trioxides XOOOX ($X = CF_3$,[16] FC(O)).[33] This last species, FC(O)OOOC(O)F, was prepared in pure state very recently.[33] Hence, for the synthesis of both matrix-isolated peroxy radicals, two different precursors were available which allowed us to perform this study.

Results and Discussion

The peroxy radicals ROO ($R = CF_3$, FC(O)) were obtained by vacuum flash pyrolysis of the thermally labile precursors $ROONO_2$ and ROOOR ($R = CF_3$, FC(O)) highly diluted in an inert gas. Typical IR matrix spectra of the pyrolysis products of the peroxy nitrates $ROONO_2$ ($R = CF_3$ or FC(O)), are depicted in Figures 1 and 2. Because the partial pressures of the precursors were $\approx 10^{-3}$ mbar and the residence times of the gas mixtures $\approx 10^{-3}$ s in the heated zone of the spray-on nozzle, predominantly the weakest bonds in $ROO-NO_2$ and ROO–OR were broken [Eqs. (4) and (5)].

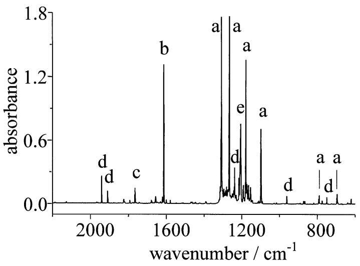

Figure 1. IR spectrum of the pyrolysis products of CF_3OONO_2 isolated in a neon matrix. Absorptions of the primary products CF_3OO and NO_2 are indicated with (a) and (b), respectively. Additional absorptions are caused by small amounts of CF_3OONO_2 (c), COF_2 (d) and CF_3O (e).

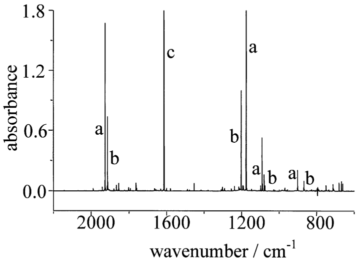

Figure 2. IR spectrum of the pyrolysis products of $FC(O)OONO_2$ isolated in a neon matrix. FC(O)OO is found as two rotamers, indicated either (a) for the *trans* or (b) for the *cis* form; (c) belongs to NO_2.

$$ROO-NO_2 \xrightarrow{\Delta} ROO + NO_2;\ R = CF_3, FC(O) \qquad (4)$$

$$ROO-OR \xrightarrow{\Delta} ROO + OR;\ R = CF_3, FC(O) \qquad (5)$$

Because of the expansion of the reaction products into a high vacuum and immediate quenching of the gas mixture on the matrix support as an inert gas matrix, secondary reactions, such as the self-reactions of the peroxy radicals or their thermal decomposition, were minimized. In the case of $R = CF_3$, formation of CF_3O radicals was observed as weak bands at 1207.9 and 1205.7 cm^{-1} in the neon matrix[34] (Figure 1). During the pyrolysis of CF_3OONO_2, trifluoromethoxy radicals are formed by the self-reaction of CF_3OO radicals according to Equation (6).

$$2\,CF_3OO \longrightarrow 2\,CF_3O + O_2 \qquad (6)$$

The greatest yields with little secondary products (such as COF_2, CO_2, CF_3O[34]) were obtained by adjusting the nozzle temperature so that the precursor was dissociated to $\approx 95\%$. For CF_3OONO_2, CF_3OOOCF_3, $FC(O)OONO_2$ and FC(O)OOOC(O)F, the optimum pyrolysis temperatures were 330, >500 (the maximum temperature allowed for the Pt-100 sensor), 310 and 230 °C, respectively. These temperatures correlate with the bond energies of 103,[35] 121,[36] 118,[37] and

0947-6539/00/0619-3646 $ 17.50+.50/0

61 kJ mol^{-1}[33] for the precursors CF_3OO-NO_2, $CF_3OO-OCF_3$, $FC(O)OO-NO_2$ and $FC(O)OO-OC(O)F$, respectively. CF_3OOOCF_3 is not an efficient precursor for CF_3OO radicals because it is too stable and it is only partially dissociated, even at 500 °C. It was found that CF_3OO is more stable than FC(O)OO and up to 500 °C no further reactions of CF_3OO, for example, the generation of CF_3 radicals, could be detected. Annealing of the argon matrices that contain the product mixtures according to Equations (4) and (5) to 35 K resulted in some reforming of the precursor molecules and concomitant changes in the matrix splitting of the IR bands, but there was no formation of new products (e.g., the tetraoxides ROOOOR, $R = CF_3$, FC(O)). The FC(O)OO radicals were formed as mixtures of two rotamers [Eq. (3)] and because the pyrolyses of the two precursors FC(O)OOOC(O)F and $FC(O)OONO_2$ were performed at different temperatures, a different rotamer ratio could be expected. Indeed, the ratios of the integrated intensities of selected IR bands for both rotamers show a small change when the reaction temperature was increased from 230 to 310 °C. An increasing amount of *cis*-FC(O)OO (in the range of 5 %) indicates that the *trans* isomer is slightly more stable.

In order to study the photochemical behaviour of both matrix-isolated peroxy radicals, the respective matrices were irradiated with light of different wavelengths. The matrix that contained FC(O)OO and FCO_2 (the latter has a strong visible absorption[31]) was irradiated with visible light from a tungsten halogen lamp; this bleached the blue matrix to colourless within minutes. The IR spectrum shows the decay of FCO_2, the formation of CO_2 and formation of no further products. The IR-inactive fluorine atoms diffused through the matrix and recombined to F_2. Further irradiation of the FC(O)OO radicals with 254 nm UV light caused the decay of all IR bands and an increase of the CO_2 and OF absorptions (Figure 3). Because the excited state of FC(O)OO in the UV region is dissociative with respect to the O–O bond (see below), the primary UV photolysis products should be $FCO_2 + O$. They can either recombine in the matrix cage to the peroxy radical or react to give $CO_2 + OF$. In addition, the photolabile FCO_2 radical can be dissociated into $F + CO_2$ and the resulting F and O atoms could recombine in the matrix cage to OF. The products CO_2 and OF are photostable with respect to photolysis at 254 nm and were observed in the IR spectra [Eq. (7)].

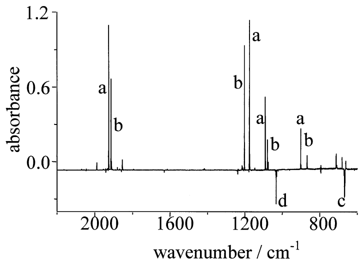

Figure 3. IR difference spectrum of the pyrolysis products of FC(O)OOOC(O)F isolated in a neon matrix before and after irradiation with UV light. The FC(O)OO absorptions [(a) for *trans*-FC(O)OO and (b) for *cis*-FC(O)OO] disappear, while CO_2 (c) and OF (d) are formed. The FCO_2 radical, which is also a pyrolysis product of the trioxide, was removed beforehand by irradiation with visible light (see text).

$$FC(O)OO + h\nu\ (254\ \mathrm{nm}) \longrightarrow [FCO_2 + O] \longrightarrow CO_2 + OF \qquad (7)$$

Irradiation of the thermolysis products of CF_3OONO_2 with unfiltered UV light from a high-pressure mercury lamp caused the decay of the CF_3OO bands, while the NO_2 bands were almost unaffected. Simultaneously, the IR bands of CF_2O and OF appeared (Figure 4). Again CF_2O and OF are the secondary recombination products of $CF_3O + O$ in the matrix cage [Eq. (8)]:

$$CF_3OO + h\nu\ (<260\ \mathrm{nm}) \longrightarrow [CF_3O + O] \longrightarrow CF_2O + OF \qquad (8)$$

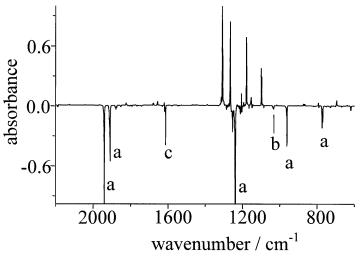

Figure 4. IR difference spectrum of the pyrolysis products of CF_3OONO_2 isolated in a neon matrix according to Figure 1 before and after irradiation with UV light. The CF_3OO absorptions (pointing upwards) disappear, while COF_2 (a) and OF (b) are formed. The NO_2 absorption (c) is caused by non-compensation.

Both photodissociation processes given in Equations (7) and (8) are thermodynamically favoured. From the heats of formation ΔH_f^{298} for CO_2 (−394), COF_2 (−639) and OF (+109 kJ mol^{-1}) given in the JANAF tables,[38] the resulting reaction enthalpies of Equations (7) and (8) are calculated to be −209 and −382 kJ mol^{-1}, respectively.

The IR spectrum of CF_3OO: A typical IR spectrum of the pyrolysis products of CF_3OONO_2, which contains CF_3OO radicals, is depicted in Figure 1. The absorptions of the byproduct NO_2 and of the secondary products, CF_2O and CF_3O,[34] are identified by reference spectra and all further bands are, for the time being, attributed to CF_3OO radicals. All those bands that decreased on UV irradiation of the matrix (Figure 4) and that were also detectable in the IR spectrum of the pyrolysis products of CF_3OOOCF_3, an independent precursor for CF_3OO, were assigned unambiguously to CF_3OO radicals and are given in Table 1. The band positions have little dependence on the matrix; solid oxygen behaves as an inert matrix material as well as the noble gases, and the neon matrix wavenumbers should be very close to the unknown gas-phase values. Assuming C_s symmetry for the CF_3OO radical, all twelve fundamentals should be IR-active according to the irreducible representation for the vibrations [Eq. (9)].

$$\Gamma_{vib} = 8\,A'\ (\mathrm{IR, Ra\,p}) + 4\,A''\ (\mathrm{IR, Ra\,dp}) \qquad (9)$$

Because the vibrational spectrum of CF_3OF,[39, 40] listed for comparison in Table 1, is similar and the O–O stretching

Table 1. IR absorptions [cm^{-1}] of band positions at the most intensive matrix site of matrix-isolated CF_3OO and their assignments.

Ne matrix			Ar matrix		O_2 matrix	CF_3OF gas[b]	assigned according to C_s symmetry		approx. description of mode
CF_3OO	int.[a]	$CF_3{}^{18}O^{18}O$	CF_3OO	$CF_3{}^{18}O^{18}O$	CF_3OO				
2606.8	0.4	2602.7	2599.1	2594.1	2598.1		$2\nu_1$	A′	
2569.6	0.2	2566.0	2560.0	2557.2	2561.1		$\nu_1+\nu_9$	A″	
2519.9	0.2		2510.5		2510.3		$2\nu_9$	A′	
2483.5	0.2		2472.2		2472.6		$\nu_1+\nu_2$	A′	
2442.3	0.3		2431.0		2431.1		$\nu_2+\nu_9$	A″	
2405.5	0.1		2394.4				$\nu_1+\nu_3$	A′	
2363.7	0.04		2353.4				$\nu_3+\nu_9$	A″	
2264.7	0.2		2257.0		2253.4		$\nu_2+\nu_3$	A′	
2187.0	0.1	2073.0	2172.2	2062.4			$2\nu_3$	A′	
1309.0	100	1306.6	1303.9	1301.8	1303.5	1294.4	ν_1	A′	ν(C–F)
1266.1	82	1263.5	1261.8	1260.5	1261.4	1262.5	ν_9	A″	ν(C–F)
1178.3	47	1168.2	1172.5	1161.4	1172.2	1223.2	ν_2	A′	ν(C–F)
1099.6	35	1043.7	1093.0	1038.2	1090.6	947.3	ν_3	A′	ν(O–O)[c]
872.7	2.2	856.8	869.2	853.9	865.3	882.1	ν_4	A′	ν(C–O)
694.8	4.6	680.6	693.2	679.2	694.2	679.0	ν_5	A′	$\delta(CF_3)$
596.9	4.6	593.0	595.2	592.3	597.4	607.5	ν_{10}	A″	$\delta(CF_3)$
495.0	1.7	488.6	491.2	485.0	488.2	584.1	ν_6	A′	$\delta(CF_3)$
449.6	0.22	439.7	447.6	438.1	448.2	441[d]	ν_7	A′	δ(COO)[c]
402.7	0.65	384.7	401.2	384.7	433.7		ν_{11}	A″	$\rho(CF_3)$
289.6	0.07	281.3	286.8	278.6		250.0	ν_8	A′	$\rho(CF_3)$
						56.0	ν_{12}	A″	τ

[a] Relative integrated intensities. [b] Ref. [39]. [c] ν(O–F) and δ(COF) for CF_3OF. [d] As shoulder in the spectrum from ref. [40.]

vibration at ≈1100 cm^{-1} is comparable to the stretching wavenumber of the O_2^- ion (≈1150 cm^{-1}), it seems that the unpaired electron in CF_3OO is localized in the OO group. The main differences in the vibrational spectra of CF_3OF and CF_3OO appear in normal modes, with a high participation of the OO or OF moiety. Because the fluorine atom has one electron more than the oxygen atom, there are specific differences in the molecular geometries of CF_3OF and CF_3OO: CF_3OF ($d_{C-O} = 1.395$ Å, $d_{O-F} = 1.421$ Å, $\sphericalangle COF = 104.8°$)[41] and CF_3OO ($d_{C-O} = 1.427$ Å, $d_{O-O} = 1.331$ Å, $\sphericalangle COO = 110.0°$).[42]

However, the vibrational spectra are only slightly affected by the change in geometry. The assignment of the fundamental vibrations of the CF_3OO radical is, for the most part, straightforward. According to Table 2, the assignment is aided by the predicted vibrational wavenumbers from ab initio calculations[28] and by the observed band positions of the ^{18}O-labelled $CF_3{}^{18}O^{18}O$ radical. The three strongest absorptions, observed at $\nu = 1309.0$, 1266.1 and 1178.3 cm^{-1} in a neon matrix, are assigned to ν_1, ν_9 and ν_2, respectively, and are described as CF stretching modes. The approximate description of ν_2 is an in-phase movement of all fluorine atoms against the C–O bond. Hence, the $^{16}O/^{18}O$ isotopic shift for this CF vibration is larger than that of the other CF stretching modes (10.1 cm^{-1} versus 2.4 cm^{-1} for ν_1 and 2.6 cm^{-1} for ν_9). The order of ν_1/ν_9 relies on the ab initio results. The band at 1099.6 cm^{-1} shows a very large isotopic shift of 45.9 cm^{-1} and is, therefore, assigned as ν(OO) or ν_3. The band at 872.7 cm^{-1} represents the fundamental ν_4 and is described approximately as ν(CO).

For all further fundamentals, except for ν_6, the band positions are within 10–20 cm^{-1} of the calculated values and the isotopic shifts are within 1 cm^{-1}. Therefore, we have unambiguously identified eleven of the twelve fundamentals of CF_3OO, two more than previously known. In addition, the results of the first excellent matrix study on CF_3OO[20] are confirmed; however, five of the earlier assignments are revised ($\nu_2 \Leftrightarrow \nu_9$; $\nu_6 \Leftrightarrow \nu_{10}$; $\nu_{11} \rightarrow \nu_8$).

Table 2. Observed and calculated wavenumbers [cm^{-1}] for the fundamental vibrations of CF_3OO.

	$CF_3{}^{16}O^{16}O$					$CF_3{}^{18}O^{18}O$			
	experimental, matrix			calcd		experimental, matrix			calcd
	Ne	Ar[a]	Ar[b]	gas[c]	gas[d]	Ne	Ar[a]	Ar[b]	gas[c]
ν_1	1309.0	1303.9	1303	1304.2	1340	1306.6	1301.5	1302	1303.0
ν_2	1178.3	1173.8	1172	1169.2	1251	1168.2	1163.5	1162	1145.0
ν_3	1099.6	1092.3	1092	1102.1	1124	1043.7	1040.1	1038	1058.1
ν_4	872.7		870	842.5	878	856.8		854	827.4
ν_5	694.8	692.8	692	671.7	686	680.6	678.9	678	657.2
ν_6	495.0		580	553.2	571	488.6		572	544.8
ν_7	449.6		448	430.0	442	439.7		440	420.7
ν_8	289.6		286	269.5	279	281.3		276	262.2
ν_9	1266.1	1263.2	1260	1266.3	1288	1263.5	1260.3	1259	1266.2
ν_{10}	596.9	597.2	597	569.7	593	593.0		594	566.2
ν_{11}	402.7			397.7	420	384.7			390.5
ν_{12}				97.7	122				93.8

[a] Ref. [22]. [b] Ref. [20]. [c] B3LYP/6-31G*, all wavenumbers scaled with 0.974, ref. [42]. [d] HF/6-31G(d), ref. [28].

The IR spectra of *cis*- and *trans*-FC(O)OO: A typical IR spectrum of the pyrolysis products of FC(O)OONO$_2$, which contains a mixture of *cis*- and *trans*-FC(O)OO radicals, is shown in Figure 2. All bands that decreased after UV irradiation (254 nm) of the matrix (Figure 3) and that were also detectable in the IR spectrum of the pyrolysis products of FC(O)OOOC(O)F—an independent precursor for FC(O)OO—unambiguously arise from FC(O)OO radicals. Assuming C_s symmetry for *cis*- and *trans*-FC(O)OO, all nine fundamentals of both rotamers should be IR-active according to the irreducible representation for the vibrations [Eq. (10)].

$$\Gamma_{\text{vib}} = 7\,\text{A}'\ (\text{IR, Ra p}) + 2\,\text{A}''\ (\text{IR, Ra dp}) \qquad (10)$$

Because a mixture of *cis*- and *trans*-FC(O)OO is formed, each fundamental appears as a doublet. The doublet components are attributed to either *cis*- or *trans*-FC(O)OO by comparison with the wavenumbers predicted by ab initio calculations[30] and by comparison with the spectra of *cis*- and *trans*-FC(O)OF.[43] Again, because the IR spectra of *cis*- and *trans*-FC(O)OF are very similar to those of *cis*- and *trans*-FC(O)OO (see Tables 3 and 4) and the O–O stretching modes near 1100 cm^{-1} are similar to the respective mode in the O$_2^-$ ion (≈1150 cm^{-1}), it can be concluded that the unpaired electron in the peroxy radicals is localized in the O–O group. According to Tables 3 and 4, the assignment of the vibrations is straightforward, and, except for the torsional modes, all fundamentals are detected. It is interesting to note that some combinations show unusually high intensities; for example, ($\nu_3+\nu_4$) in both radicals is strongly increased in intensity by Fermi resonance with ν_1.

The electronic spectra of CF$_3$OO and FC(O)OO: The interaction of the unpaired electron of a radical R$^\bullet$ with one of the two unpaired π* electrons of an oxygen molecule has been described in a simple molecular orbital diagram for ROO radicals.[1] The σ(R–O) bond is formed at the expense of the (O=O) bond, reducing this from double to a lower bond order. The extent of the bond weakening is dependent on the nature of the substituent R. For example, if R is CH$_3$ or Cl, the bond order becomes 1.5[1] or 1.9[44, 45], respectively. Because in ROO the unpaired electron occupies an out-of-plane, oxygen π* orbital, the electronic ground state is of ^{2}A″ symmetry. Promotion of an electron either from the in-plane oxygen lone-pair into the π* out-of-plane orbital (X^{2}A″ → 1^{2}A′, n → π* transition) or from the out-of-plane π-orbital into the out-of-plane π*-orbital (X^{2}A″ → 2^{2}A″, π → π* transition) causes absorptions in the near-IR and UV region, respectively. The excited state in the near-IR region should be bound because the electronic absorption spectra of organic peroxy radicals exhibit characteristic O–O stretching progressions.[46] We intended to measure the unknown near-IR spectra of matrix-isolated CF$_3$OO and FC(O)OO. However, in spite of the quite high concentrations in the matrices (absorbance units in the UV and IR region were between 0.5 and 2) no absorption could be detected in the spectral region 5000–30 000 cm^{-1} (where the noise level was 0.01 to 0.03 absorbance units).

The excited 2^{2}A″ state is antibonding in the O–O coordinate of organic peroxy radicals; this is consistent with the broad, featureless appearance of the absorption bands, typically in the range 200 to 250 nm.

Table 3. IR absorptions [cm^{-1}] (of band positions at the most intensive matrix sites) in matrix-isolated *trans*-FC(O)OO and their assignments.

Ne matrix	Int.[a]	Ar matrix	Calcd[b]	Int.[a]	*trans*-FC(O)OF[c]	assigned according to C_s symmetry		approx. description of mode
3831.2	1.0	3817.6			3826.8	$2\nu_1$	A′	
3090.6	0.2					$\nu_1+\nu_2$	A′	
3011.8	0.1				2907.3	$\nu_1+\nu_3$	A′	
2824.2	0.3	2811.9			2827.9	$\nu_1+\nu_4$	A′	
2341.2	1.3	2327.4			2351.9	$2\nu_2$	A′	
2259.3	0.4				2160.8	$\nu_2+\nu_3$	A′	
2162.8	0.2				1974.0	$2\nu_3$	A′	
2069.5	1.4	2057.4			2083.5	$\nu_2+\nu_4$	A′	
1988.9	4.0	1978.5			1889.9	$\nu_3+\nu_4$	A′	
1925.9	85	1919.2	1964	100[d]	1924.5	ν_1	A′	ν(C=O)
1880.0	0.9	1873.8				ν_1	A′	ν(^{13}C=O)
1850.9	0.3	1841.9			1829.7	$\nu_2+\nu_5$	A′	
1793.8	0.6					$2\nu_4$	A′	
1690.4	0.1					$\nu_2+\nu_6$	A′	
1416.4	2.2	1408.1			1409.9	$\nu_4+\nu_6$	A′	
1360.1	0.2				1306.1	$2\nu_5$	A′	
1211.0	1.5	1209.7			1156.1	$\nu_5+\nu_6$	A′	
1175.0	100	1168.3	1176	62	1181.1	ν_2	A′	ν(C–F)
1146.0	1.1	1139.6				ν_2	A′	ν(^{13}C–F)
1090.1	38	1084.8	1128	60	990.2	ν_3	A′	ν(O–O)[e]
900.8	23	895.7	890	18	908.2	ν_4	A′	ν(C–O)
712.0	9.1	707.4	700	9.2	739.1	ν_8	A″	γ(FCOO$_2$)[e]
680.2	3.7	678.4	675	1.8	653.5	ν_5	A′	δ(O=C–O)
520.9	1.5	518.5	512	0.5	503.6	ν_6	A′	δ(F–C=O)
335.7	0.7		326	0.8	304.8	ν_7	A′	δ(C-O-O)[e]
			114	0.0	193.4	ν_9	A″	τ

[a] Relative integrated absorbances. [b] B3LYP/6-31 + G(d)/B3LYP/6-31 + G(d) + ZPC, ref. [30]. [c] Ar matrix, ref. [43]. [d] Absolute intensity 363 km mol^{-1}, ref. [30]. [e] ν(O–F), γ(FCOOF), δ(C-O-F) for FC(O)OF.

Table 4. IR absorptions [cm^{-1}] (of band positions of the most intensive matrix sites) of matrix-isolated *cis*-FC(O)OO and their assignments.

Ne matrix	Int.[a]	Ar matrix matrix	Calcd[b]	Int.[a]	*cis*-FC(O)OF[c]	assigned according to C_s symmetry		approx. description of mode
3808.2	0.4	3790.0			3779.8	$2\nu_1$	A′	
3110.4	0.1					$\nu_1+\nu_2$	A′	
2392.8	0.3				2493.7	$2\nu_2$	A′	
2279.0	0.4				2174.2	$\nu_2+\nu_3$	A′	
2139.4	0.3				1851.3	$2\nu_3$	A′	
2057.0	0.7	2047.7			2109.0	$\nu_2+\nu_4$	A′	
1942.2	7.1	1931.6				$\nu_3+\nu_4$	A′	
1913.2	100	1904.5	1944	100[d]	1895.7	ν_1	A′	ν(C=O)
1868.0	1.0	1860.0				ν_1	A′	ν(^{13}C=O)
1853.7	7.1	1846.4			1865.2	$\nu_2+\nu_5$	A′	
1752.5	0.3				1781.9	$\nu_2+\nu_6$	A′	
1214.2	4.2	1204.9				$\nu_5+\nu_6$	A′	
1202.1	83	1196.7	1199	76	1253.7	ν_2	A′	ν(C–F)
1172.5	0.9					ν_2	A′	ν(^{13}C–F)
1078.1	15	1071.9	1114	25	929.8	ν_3	A′	ν(O–O)[e]
867.1	20	863.6	860	14	861.1	ν_4	A′	ν(C–O)
708.7	5.0	704.2	699	9.8	733.0	ν_8	A″	γ(FCOO$_2$)[e]
661.0	5.8	659.2	661	4.0	626.3	ν_5	A′	δ(O=C–O)
552.7	1.1	550.3	546	0.8	530.1	ν_6	A′	δ(F–C=O)
346.4	0.7		337	0.5	315.8	ν_7	A′	δ(C-O-O)[e]
			118	0.2	154.1	ν_9	A″	τ

[a] Relative integrated absorbances. [b] B3LYP/6-31+G(d)/B3LYP/6-31+G(d)+ZPC, ref. [30]. [c] Ar matrix, ref. [43]. [d] Absolute intensity 379 km mol^{-1}, ref. [30]. [e] ν(O–F), γ(FCOOF), δ(C-O-F) for FC(O)OF.

The shape of the absorption bands can be simulated by a Gaussian function [Eq. (11)][1], in which λ_{max} represents the

$$\sigma_\lambda = \sigma_{max} \exp\{-\alpha[\ln(\lambda_{max}/\lambda)]^2\} \qquad (11)$$

wavelength of the absorption maximum σ_{max} and α is a measure of the width of the absorption profile.

The Gaussian profile is a consequence of the Franck–Condon principle for the transition from a bound ground state to a repulsive, excited electronic state.

Because the strong UV absorptions are used for quantitative kinetic experiments, the cross-sections of the absorption profiles are of fundamental importance. The reported cross-section data for CF_3OO[18, 19] and FC(O)OO[2, 17], gathered in Tables 5 and 6, were obtained by flash photolysis/time-resolved UV spectroscopy of $F_2/CF_3H/O_2$ or $F_2/CO/O_2$ mixtures or pulse radiolysis/transient UV spectroscopy of $SF_6/CF_3H/O_2$ or $SF_6/CO/O_2$ mixtures. Here we describe a new independent route for the determination of the absorption cross-sections by matrix-isolation experiments. The final UV spectra of the radicals CF_3OO (Figure 5) and FC(O)OO (Figure 6) were evaluated from the UV spectra of the matrix-isolated pyrolysis products of the corresponding peroxy nitrates CF_3OONO_2 and FC(O)OONO$_2$, respectively; Figure 7 illustrates the procedure. It is assumed that the peroxy and NO_2 radicals are formed in equimolar ratios during vacuum flash pyrolysis. In the resulting mixtures, NO_2 is the only absorber in the spectral region 300–375 nm (Figure 7,

Table 5. Absorption cross-sections of CF_3OO.

Wavelength [nm]	σ [10^{-20} cm^2] this work	Maricq, Szente[a]	Nielsen et al.[b]
200	160	377	
205	201	412	
206.5[c]	207	421	
210	196	427	
215	189	417	340
220	170	376	297
225	141	317	267
230	110	252	206
235	79	190	162
240	51	130	127
245	30	88	101
250	16	53	66
255	6	33	41
260		20	25

[a] Ref. [18], the literature values are interpolated to the wavelength given in the first column. [b] Ref. [19], value at $\lambda = 255$ nm interpolated. [c] Maximum of absorbance.

Table 6. Absorption cross-sections of FC(O)OO.

Wavelength [nm]	σ [10^{-20} cm^2] this work	Maricq, Francisco[a]	Wallington et al.[b]
200	186	269	
205	115	217	
210	108	219	
215	130	246	
220	152	268	272
225	169	290	315
230	184	298	297
235[c]	188	290	301
240	181	277	269
245	163	249	264
250	139	216	213
255	111	181	181
260	85	148	155
265	61	108	117
270	41	82	83
275	25	59	66
280	15	31	41
285	7	24	26
290	3	20	19

[a] Ref. [17], the literature values are interpolated to the wavelength given in the first column. [b] Ref. [2]. [c] Maximum of absorbance.

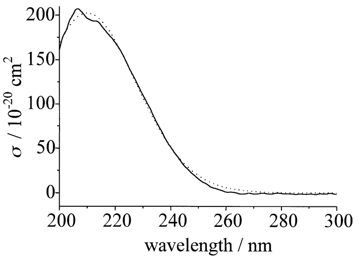

Figure 5. UV spectrum of CF_3OO isolated in a neon matrix (solid line). The dashed line fits the spectrum to a Gaussian line-shape (see text).

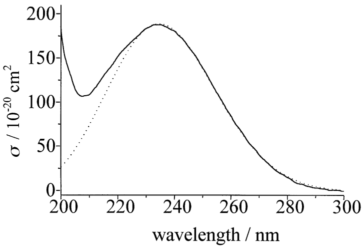

Figure 6. UV spectrum of FC(O)OO isolated in a neon matrix (solid line). The dashed line fits the spectrum to a Gaussian line-shape (see text).

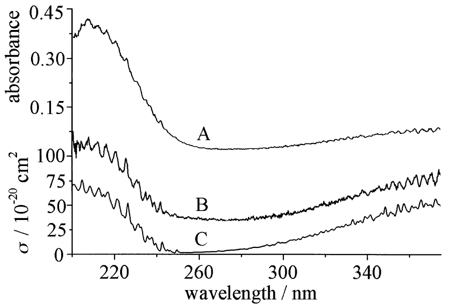

Figure 7. Evaluation of the UV spectrum of CF_3OO. Spectrum A shows the absorptions of the pyrolysis products of CF_3OONO_2 isolated in a neon matrix. Spectrum B is obtained from NO_2 isolated in a neon matrix. The matrix was deposited under the same conditions as the pyrolysis products resulting in spectrum A. The cross-sections for B were adjusted to those of NO_2 measured in the gas phase (spectrum C). B is shown with an offset of 25 × 10^{-20} cm^2. The CF_3OO spectrum (Figure 5) is obtained by subtracting B from A.

spectrum A). This structured spectrum can be used to convert absorbances into cross-section units. For this purpose, a gas-phase spectrum of NO_2 was recorded under the same registration conditions as spectrum A (Figure 7, spectrum C) and the cross-sections (base e) were determined according to Equation (12), in which T = temperature [K], p = pressure [mbar] and d = optical path length [cm].

$$\sigma = 31.79 \log(I_o/I) T p^{-1} d^{-1} \; [10^{-20}\,\mathrm{cm}^2] \qquad (12)$$

By adjusting spectrum A to C in the spectral region of 300–375 nm, a scaling factor of (890 × 10^{-20} cm^2 per absorption unit) is obtained for the conversion of the matrix absorbance into the cross-section scale.

This procedure requires that the changes of the spectra for NO_2 and peroxy radicals are comparable (relatively small and parallel) when going from the gas-phase to matrix-isolated species and vice versa. For example, this approach was applicable for OClO and ClOO isolated in a neon matrix.[44] In order to eliminate the NO_2 bands from spectrum A (Figure 7), a reference spectrum (B) of NO_2 isolated in a neon matrix was subtracted. The result is displayed in Figure 5 and the absorption cross-sections are listed in Tables 5 and 6. Equation (11) was used to calculate $\lambda_{max} = 209.8 \pm 1$ nm, $\alpha = 75.8 \pm 0.6$ and $\sigma_{max} = 203 \pm 1\; 10^{-20}$ cm^2 for CF_3OO. The FC(O)OO spectrum can be simulated with $\lambda_{max} = 234.6 \pm 0.1$ nm, $\alpha = 76.0 \pm 0.3$ and $\sigma_{max} = 190 \pm 1\; 10^{-20}$ cm^2. For CF_3OO and FC(O)OO, σ_{max} values are lower by about 50 and 30 %, respectively, than the published data.[18, 19, 2, 17] The position of the maximum absorbances λ_{max} and their band widths are in agreement with the literature data. These deviations in the absorption cross-sections and the differences presented in Tables 5 and 6 are caused by systematic errors. Firstly, the absorption cross-section can be influenced by the matrix material. However, gas phase and solution absorption cross-sections (in inert solvents) agree, in general, within 10 %. Because solid neon can be viewed as a very weak interacting solvent, the change in the absorption cross-section should be smaller than 5 %. Secondly, the postulated 1:1 ratio of peroxy radicals to NO_2 is changed by secondary reactions of the peroxy radicals. Indeed, in the IR spectra of the pyrolysis products CO_2, COF_2 and CF_3O were observed as impurities. For CF_3OO, a decomposition of 5–10 % can be estimated from secondary products. Therefore, the concentration of CF_3OO was overestimated by 5–10 %, which leads to an equivalent underestimation of the absorption cross-sections. Thirdly, the subtraction procedure leads to a small statistical error. For these reasons we quote an error of +20/−10 % for the values of CF_3OO (Table 5) and of FC(O)OO (Table 6). As the differences between our data and that given in the literature increase with increasing wavelength, it can be supposed that these differences are caused by additional absorptions of side-products from the initiating radicals SF_5 or F in the previous studies. Transient species, such as FOO, SF_5OO, FCO, FCO_2 or ROOOOR, may be formed which lower the concentration of the peroxy radicals and partially interfere with their UV spectra. Further efforts to eliminate these discrepancies are desirable.

The different bonding situations at the carbon atoms in CF_3OO and FC(O)OO are responsible for the varying positions of the absorption maxima.

The $X^2A'' \rightarrow 2^2A''$ transition (π → π*, both out-of-plane) is only influenced by other A″-type orbitals of the radicals. In the CF_3OO radical, only the occupied, non-bonding A″-type orbitals, mainly located on the F atoms of the CF_3 group, interact with the A″-type orbitals of the peroxy group: this interaction is expected to be small. In the FC(O)OO radical the π system of the carbonyl group includes an occupied bonding A″-type orbital and an unoccupied A″ orbital, which is mainly located at the carbon atom. This unoccupied A″ orbital is expected to give strong interactions with the A″-type orbital of the peroxy group. The stronger influence on the A″-type orbital of the peroxy group in FC(O)OO lowers the transition energy between the X^2A'' and the $2^2A''$ state with respect to CF_3OO. Therefore, the corresponding UV absorption band of the FC(O)OO radical is found at longer wavelengths than that of the CF_3OO radical.

Experimental Section

The peroxy nitrates ROONO$_2$ and trioxides ROOOR, R = CF$_3$, FC(O), are potentially explosive, especially in the presence of oxidisable materials. It is important to take safety precautions when these compounds are handled in the liquid or solid state. Reactions involving either one of these species should only be carried out in millimolar quantities.

General procedures and reagents: Volatile materials were manipulated in a glass vacuum-line equipped with two capacitance pressure gauges (221 AHS-1000 and 221 AHS-10, MKS Baratron, Burlington, MA), three U-traps and valves with PTFE stems (Young, London, (UK)). The vacuum line was connected to an IR cell (optical path length 200 mm, Si windows 0.5 mm thick) contained in the sample compartment of the FTIR instrument. This allowed us to observe the purification processes and to follow the course of reactions. The thermally labile compounds FC(O)OONO$_2$,[6] CF$_3$OONO$_2$,[7] CF$_3$OOOCF$_3$[16] and FC(O)OOOC(O)F[33] were prepared according to literature procedures and stored in flame-sealed glass ampoules under liquid nitrogen in a long-term Dewar vessel. The ampoules were opened with an ampoule key[47] on the vacuum line, an appropriate amount was taken out for the experiments and then they were flame-sealed again. The following chemicals were obtained from commercial sources: CF$_3$I (Kali-Chemie, now Solvay, Hannover (Germany)) and NO$_2$ (99% Baker, Philipsburg, NY). They were purified by trap-to-trap condensation prior to use. ^{18}O$_2$ (>99%, Ventron, Numbai (India)), O$_2$ (99.999%, Linde, Munich (Germany)), Ar (99.999%, Messer Griesheim, Krefeld (Germany)) and Ne (>99.99%, Messer Griesheim) were used without further purification. According to the literature,[7] the synthesis of the isotopically labelled CF$_3$^{18}O^{18}ONO$_2$ is accomplished by the reaction of photolytically generated CF$_3$ radicals with ^{18}O$_2$ and NO$_2$ in a modified procedure. For this purpose an evacuated 90 mL quartz reactor was loaded with CF$_3$I (0.20 mmol) and NO$_2$ (0.18 mmol), and then filled with ^{18}O$_2$ up to 900 mbar. Subsequently, the quartz reactor was placed in a transparent quartz Dewar vessel containing ice-water and irradiated with a 15 W low pressure mercury lamp (TK15, Heraeus, Hanau (Germany)). After a reaction time of 4 h at 0 °C, the reactor was cooled to -196 °C and the excess ^{18}O$_2$ (contaminated with some ^{16}O^{18}O, from partial equilibration of ^{18}O$_2$ with unlabelled NO$_2$) was recovered by cryopumping the oxygen into a vessel filled with molecular sieves (5 Å) held at -196 °C. The crude product was separated by repeated trap-to-trap condensation in vacuo in a series of traps held at -100, -120 and -196 °C. The trap held at -120 °C retained CF$_3$^{18}O^{18}ONO$_2$ contaminated with NO$_2$ and CF$_3$I.

Preparation of matrices: Small amounts of the samples ($\approx$0.1 mmol) were transferred in vacuo into a small U-trap immersed in liquid nitrogen. This U-trap was mounted in front of the matrix support (a metal mirror) and maintained at a temperature of -140 °C (isopentane bath) for CF$_3$OONO$_2$, -125 °C (isopentane bath) for FC(O)OONO$_2$ and -95 °C (ethanol bath) for FC(O)OOOC(O)F. A gas stream ($\approx$3 mmol h^{-1}) of argon, oxygen or neon was directed over the cold sample in the U-trap, and the resulting gas mixtures passed the heated quartz nozzle (4 mm internal diameter, with an end orifice of 1 mm) within milliseconds and were subsequently quenched on the matrix support at 12 or 5 K. Because the vapor pressures of the samples in the cold U-trap were $\approx 10^{-3}$ mbar and the pressures of the inert gas streams during the deposition were $\approx$1 mbar in the U-trap, the resulting sample-to-gas ratios can be estimated to be 1:1000. For each sample, two different amounts of matrix material (1 and 3 mmol) were deposited through the heated nozzle at temperatures of 330 °C (CF$_3$OONO$_2$), 500 °C (CF$_3$OOOCF$_3$), 310 °C (FC(O)OONO$_2$) and 220 °C (FC(O)OOOC(O)F). The mixtures of NO$_2$:Ne (1:1000) or CF$_3$OOOCF$_3$:Ne (1:500) were prepared in a stainless steel high-vacuum line, transferred by means of a stainless steel capillary to the heated nozzle, and quenched as a matrix at 5 K.

Photolysis experiments on the matrices were undertaken in the visible and UV regions with a 250 W tungsten halogen lamp (Osram, Munich (Germany)) or a high-pressure mercury lamp (TQ 150, Heraeus, Hanau (Germany)), respectively, in combination with cut-off and interference filters (Schott, Mainz (Germany)). Details of the matrix apparatus have been described elsewhere.[31]

Instrumentation

IR spectroscopy: Gas-phase infrared spectra were recorded with a resolution of 2 cm^{-1} in the range $\nu = 4000-400$ cm^{-1}, on a FTIR instrument (Nicolet, Impact 400 D, Madison WI), which was directly coupled with the vacuum line. Matrix IR spectra were recorded on a IFS 66v/S FT spectrometer (Bruker, Karlsruhe (Germany)) in the reflectance mode with a transfer optic. A DTGS or MCT detector together with a KBr/Ge beam splitter operated in the regions $\nu = 5000-400$ or $7000-600$ cm^{-1}, respectively. In these regions, 64 scans were co-added for each spectrum by means of apodized resolutions of 1.0 or 0.2 cm^{-1}. A far-IR DTGS detector together with a Ge-coated 6 µm Mylar foil beam-splitter was used in the region $650-80$ cm^{-1}. In this region 64 scans were co-added for each spectrum by means of an apodized resolution of 1.0 cm^{-1}.

UV spectroscopy: UV spectra were recorded in the region $\lambda = 200-2000$ nm with a Lambda 900 instrument (Perkin–Elmer, Norwalk, CT) and a spectral resolution of 0.5 nm. For matrix measurements, two quartz single fibers of 2 m length with a special condenser (Hellma, Jena (Germany)) were used and the gas-phase UV spectrum of NO$_2$ was recorded in a gas cell with a 10 cm optical path length.

Acknowledgements

Financial support by the Deutsche Forschungsgemeinschaft and the Fonds der Chemischen Industrie is gratefully acknowledged.

---

[1] J. S. Francisco, M. M. Maricq in *Advances in Photochemistry, Vol. 20* (Eds.: D. C. Neckers, D. H. Volman, G. von Bünau), Wiley, New York, **1995**, pp. 79–163.

[2] T. J. Wallington, T. Ellermann, O. J. Nielsen, J. Sehested, *J. Phys. Chem.* **1994**, *98*, 2346.

[3] T. J. Bevilacqua, D. R. Hanson, C. J. Howard, *J. Phys. Chem.* **1993**, *97*, 3750.

[4] A. A. Turnipseed, S. B . Barone, A. R. Ravishankara, *J. Phys. Chem.* **1994**, *98*, 4594.

[5] H. Niki, J. Chen, V. Young, *Res. Chem. Intermed.* **1994**, *20*, 277.

[6] D. Scheffler, I. Schaper, H. Willner, H.-G. Mack, H. Oberhammer, *Inorg. Chem.* **1997**, *36*, 339.

[7] R. Kopitzky, H. Willner, H.-G. Mack, A. Pfeiffer, H. Oberhammer, *Inorg. Chem.* **1998**, *37*, 6208.

[8] P. Biggs, C. E. Canosa-Mas, J.-M. Fracheboud, C. J. Percival, R. P. Wayne, D. E. Shallcross, *J. Chem. Soc. Faraday Trans.* **1997**, *93*, 379.

[9] R. Meller, G. K. Moortgat, *J. Photochem. Photobiol. A* **1995**, *86*, 15.

[10] M. K. W. Ko, N.-D. Sze, J. M. Rodriguez, D. K. Weistenstein, C. W. Heisey, R. P. Wayne, P. Biggs, C. E. Canosa-Mas, H. W. Sidebottom, J. Treacy, *Geophys. Res. Lett.* **1994**, *21*, 101.

[11] A. R. Ravishankara, A. A. Turnipseed, N. R. Jensen, S. Barone, M. Mills, C. J. Howard, S. Solomon, *Science* **1994**, *263*, 71.

[12] *Scientific Assessment of Stratospheric Ozone, WMO Report No. 20, Vol. 2*, Appendix, AFEAS report, **1989**.

[13] *Scientific Assessment of Stratospheric Ozone, WMO Report No. 25*, **1991**.

[14] J. M. Heras, A. J. Arvia, P. J. Aymonino, H. J. Schumacher, *Z. Phys. Chem.* **1961**, *28*, 250.

[15] A. J. Arvia, P. J. Aymonino, H. J. Schumacher, *Z. Anorg. Allg. Chem.* **1962**, *316*, 327.

[16] E. L. Varetti, P. J. Aymonino, *An. Asoc. Quim. Argent.* **1970**, *58*, 23.

[17] M. M. Maricq, J. J. Szente, G. A. Khitrov, J. S. Francisco, *J. Chem. Phys.* **1993**, *98*, 9522.

[18] M. M. Maricq, J. J. Szente, *J. Phys. Chem.* **1992**, *96*, 4925.

[19] O. J. Nielsen, T. Ellermann, J. Sehested, E. Bartkiewicz, T. J. Wallington, M. D. Hurley, *Int. J. Chem. Kinet.* **1992**, *24*, 1009.

[20] R. Butler, A. Snelson, *J. Phys. Chem.* **1979**, *83*, 3243.

[21] K. C. Clemitshaw, J. R. Sodeau, *J. Phys. Chem.* **1987**, *91*, 3650.

[22] K. C. Clemitshaw, J. R. Sodeau, *J. Phys. Chem.* **1989**, *93*, 3552.

[23] C. Mohua, W. Xuefeng, Y. Min, Q. Qizong, Z. Qike, *Chinese J. Chem. Phys.* **1998**, *11*, 37.

[24] T. J. Wallington, M. D. Hurley, M. M. Maricq, *Chem. Phys. Lett.* **1993**, *205*, 62.

[25] S. I. Ahonkhai, A. Nölle, P. Behr, H. Heydtmann, *J. Photochem. Photobiol. A* **1994**, *80*, 389.

[26] G. Bednarek, G. A. Argüello, R. Zellner, *Ber. Bunsenges. Phys. Chem.* **1996**, *100*, 445.

[27] W. F. Schneider, T. J. Wallington, *J. Phys. Chem.* **1993**, *97*, 12783.

[28] M. R. Zachariah, P. R. Westmoreland, D. R. Burgess, Jr., W. Tsang, C. F. Melius, *J. Phys. Chem.* **1996**, *100*, 8737.

[29] M. P. Badenes, E. Castellano, C. J. Cobos, A. E. Croce, M. E. Tucceri, *Chem. Phys. Lett.* **1999**, *303*, 482.

[30] M. L. McKee, T. R. Webb, *J. Phys. Chem.* **1996**, *100*, 11292.

[31] G. A. Argüello, H. Grothe, M. Kronberg, H. Willner, H.-G. Mack, *J. Phys. Chem.* **1995**, *99*, 17525.

[32] H. Grothe, H. Willner, *Angew. Chem.* **1994**, *106*, 1581; *Angew. Chem. Int. Ed. Engl.* **1994**, *33*, 1482.

[33] H. Pernice, H. Willner, M. L. McKee, T. R. Webb, unpublished results.

[34] G. A. Argüello, H. Willner, unpublished results.

[35] K. H. Becker, A. Mayer-Figge, *Berichte der Bergische Universität Gesamt Hochschule Wuppertal* **1997**, *42*, 54; A. Mayer-Figge, F. Zabel, K. H. Becker, *J. Phys. Chem.* **1996**, *100*, 6587.

[36] J. S. Francisco, I. H. Williams, *Int. J. Chem. Kinet.* **1988**, *20*, 455.

[37] T. J. Wallington, W. F. Schneider, T. E. Møgelberg, O. J. Nielsen, J. Sehested, *Int. J. Chem. Kinet.* **1995**, *27*, 391.

[38] M. W. Chase, Jr., C. A. Davies, J. R. Downey, Jr., D. J. Frurip, R. A. McDonald, A. N. Syverud, *JANAF Thermochemical Tables*, 3rd ed. American Institute of Physics, New York, **1985**.

[39] P. M. Wilt, E. A. Jones, *J. Inorg. Nucl. Chem.* **1967**, *29*, 2108.

[40] R. T. Lagemann, E. A. Jones, P. J. H. Woltz, *J. Chem. Phys.* **1952**, *20*, 1768.

[41] F. P. Diodati, L. S. Bartell, *J. Mol. Struct.* **1971**, *8*, 395.

[42] H. Oberhammer, private communication.

[43] G. A. Argüello, B. Jülicher, S. E. Ulic, H. Willner, B. Casper, H.-G. Mack, H. Oberhammer, *Inorg. Chem.* **1995**, *34*, 2089.

[44] H. S. P. Müller, H. Willner, *J. Phys. Chem.* **1993**, *97*, 10589.

[45] H. Siebert, *Anwendungen der Schwingungsspektroskopie in der anorganischen Chemie,* Springer, Berlin, **1966**, p. 36.

[46] H. E. Hunziker, H. R. Wendt, *J. Chem. Phys.* **1976**, *64*, 3488.

[47] W. Gombler, H. Willner, *J. Phys. E* **1987**, *20*, 1286.

Received: February 4, 2000 [F2280]